ARTICLE

Trends and Temporal of Rainfall Erosion due Variability Rainfall in Nakambè Watershed, Burkina Faso

Joseph Yaméogo [1*] [ID] *, Songanaba Rouamba* [2] [ID] *, Suzanne Koala* [2] [ID] *, Richard Zongo* [2] [ID]

[1]*Department of Human Sciences and Society, Ziniaré University Center/Joseph KI-ZERBO University, Ouagadougou 7021, Burkina Faso*

[2]*Department of Geography, Norbert ZONGO University, Koudougou 376, Burkina Faso*

ABSTRACT

Understanding how rain erosion evolves and what determines it can contribute to the better management of soil resources. This study analyses the evolution of rain erosion in the Nakambè catchment in Burkina Faso between 1992 and 2022. Monthly rainfall data for this period were extracted from NASA POWER. Erodibility indices were then employed to evaluate the extent of erosion. Precipitation variability was assessed using the coefficients of variation and the standardized precipitation index. The study shows that precipitation varied within the catchment area during this period. This variation is seasonal, as it fluctuates before, during and after the rainy season, with a coefficient of variation ranging from 18 during the rainy season to 556.18 after the rainy season. The catchment also exhibits multi-year fluctuations, long-term fluctuations or perennial variations (1992–2004 and 2004–2022). The study also shows that rain erosion varies annually and seasonally. The Fournier, Arnoldus and rainfall concentration indices indicate variability in erosivity, with a significant increase in August. It also appears that rainfall trends and variability have an impact on erosion in the catchment. For example, erosion increases with precipitation concentration and the standardized rainfall anomaly over the period 1992-2022. The cumulative effect of precipitation concentration—reflected in increased rainfall during July and August—along with the wet phase of the 1992–2022 period, are the main determining factors for rain erosion in the catchment. It is therefore important to limit the construction of dams in the basin, as they may contribute to the continued degradation of the catchment.

Keywords: Nakambé Watershed; Rainfall Variability; Erosion Index Trends, Burkina Faso

*CORRESPONDING AUTHOR:

Joseph Yaméogo, Department of Human Sciences and Society, Ziniaré University Center/Joseph KI-ZERBO University, Ouagadougou 7021, Burkina Faso; Email: josephyameogo10@gmail.com; joseph.yameogo@ujkz.bf

1. Introduction

The Sudano-Sahelian zone of West Africa is subject to climatic variability over periods of thousands of years [1], hundreds of years [2] and decades [3]. This situation has implications for natural resources in this part of Africa. The situation in several catchments is of concern because of the changes in ecosystems caused by the interactions between climate and human activities. Several studies have been carried out on the different catchments in West Africa. The Benue catchment in Nigeria [4], the Tordzie and Vea catchments in Ghana [5,6], the Nouhao sub-catchment [7] and the Vranso sub-catchment [8] are all experiencing spatial and temporal changes in temperature and precipitation extremes, leading to an increased occurrence of extreme events in these areas. This is particularly true for the dynamics of land use in the Cavally River basin in Toulepleu, Côte d'Ivoire [9], the unavailability of water resources in the transboundary Sassandra basin [10], the disruption of water flow in the Bénoué basin in northern Cameroon [11], the Mekrou basin [12], and the increased vulnerability of riparian populations in the Comoé basin [13].

The impact of global warming on rainfall patterns may lead to major changes in rainfall erosivity, both in terms of annual values and seasonal distribution [14,15]. But, very few studies on this subject have been conducted in West Africa, particularly in Burkina Faso. Of those that have been conducted, many have focused on water resource availability in the Nakambè and Mouhoun basins [16–18], as well as on extreme rainfall trends in the Nakambè.

however, the Nakambè catchment area is essential for the development of Burkina Faso. Several hydro-agricultural dams have been built there. These include the Bagré dam, which has a capacity of 1.7 billion cubic meters and is used for both electricity generation and irrigation. The Ziga dam, with a capacity of 200 million cubic meters, is intended to supply drinking water to urban populations. The Toecé dam, with a capacity of 75 million cubic meters, is intended for hydro-agricultural use. The Guiti dam has a capacity of 44 million cubic meters and is intended to supply the local population with drinking water. Due to the demand for water for multiple uses, such as electricity generation, agriculture, fishing, livestock farming and drinking water supply, the Nakambè is in particularly high demand.

Insufficient knowledge of the extent and causes of rainfall erosion in the Nakambè basin can lead to unsustainable agricultural practices, dyke damage and soil erosion. This can jeopardise the basin's long-term sustainability. Understanding temporal trends in rainfall variability and erosion can inform the development of sustainable environmental planning policies. The study's primary objective is therefore to analyse rainfall and erosion variability in the Nakambè catchment between 1992 and 2022.

2. Materials and Methods

2.1. Study Area

Burkina Faso is located in the Sudano-Sahelian zone of West Africa. It has four watersheds: those of the Comoé, Mouhoun, Nakambè and Niger rivers (**Figure 1**).
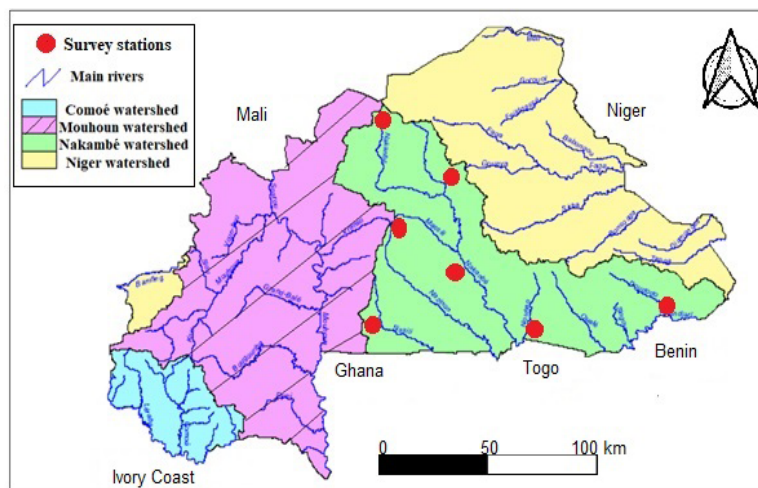

Figure 1. Location of the Nakambè watershed.

2.2. Data Source

They are based on data provided by NASA's Langley Research Center (LaRC) as part of the Prediction of Worldwide Energy Resource (POWER) project, funded by NASA's Earth Science/Applied Science programme. The data are based on satellite observations from which surface insolation values are derived. They are also based on a global grid with a resolution of 0.5° latitude by 0.5° longitude. The data were downloaded from https://power.larc.nasa.gov/data-access-viewer/. Mean precipitation data were extracted at monthly intervals over the period 1992–2022. There are several reasons to use NASA Prediction of Worldwide Energy Resources (POWER) data. Ground measurements are still rare and unevenly distributed, particularly in developing countries such as Burkina Faso. Furthermore, when they are available, they are expensive to acquire, which prevents appropriate studies on catchment areas from being carried out. Satellite-derived rainfall estimates are an alternative, but their accuracy must first be validated. However, there are no rainfall data available for the period between 1992 and 2022. It is therefore difficult to evaluate these data. Nevertheless, the research [19] demonstrate that NASA POWER data can accurately capture climatological precipitation patterns in tropical regions. In the arid and semi-arid zones of Jordan [20] demonstrated significant correlations between NASA POWER data and ground measurements, with relatively high R values (0.67–0.91), especially when annual rainfall exceeds 50 mm. This data has already been used to analyse extreme temperatures in Burkina Faso [21] and rainfall in the Dano catchment [22]. Other studies in West Africa, such as [23,24], have also utilised these data. **Table 1** below summarises the characteristics of the selected stations.

Table 1. Characteristics of the selected stations.

No.	Name of locality	Period selected	Climatic domain	Latitude	Longitude	Altitudes
1	Tambarga	1992–2022	Sudanese	11.4675	1.3788	201.88 m
2	Kompienga	1992–2022	Sudanese	11.0283	0.6665	198.59 m
3	Gosina	1992–2022	Sudano-Sahelian	12.5145	–2.843	283.4 m
4	Dadounin	1992–2022	Sudano-Sahelian	11.1344	–2.7005	291.18 m
5	Sinikiere	1992–2022	Sudano-Sahelian	11.804	–0.9537	297.09 m
6	Toyandé	1992–2022	Sahelian	13.2775	–1.1646	320.11 m
7	Sole	1992–2022	Sahelian	14.1211	–2.0918	321.77 m

Source: https://power.larc.nasa.gov/data-access-viewer/.

2.3. Methods

They are concerned with methods for the analysis of variability and trends in precipitation and rain erosion.

2.3.1. Methods to Analyze Rainfall Variability

The coefficient of variation (CV) and the standard rainfall anomaly (SRA) are used to study the inter- and intra-annual variability of climatic variables [25–28]. A moving average has also been added in order to give a clearer picture of the variability.

- **Standardised rainfall anomaly (SRA)**

This index provides an indication of inter-annual rainfall variability in the study area over the observation period [29]. It is the difference between the long-term average rainfall (sometimes called the reference value) and the annual rainfall in a given year, divided by the standard deviation [30]. Its mathematical formula is defined as follows [31]:

$$Z = \frac{x_i - \mu}{\sigma} \qquad (1)$$

where Z is SRA; x_i is the annual rainfall for a particular year; μ is the long-term average annual precipitation over an observation period (1992–2022); σ is the standard deviation of annual precipitation over the observation period (1992–2022).

The SRA classifications and interpretations are sum-

marised in **Table 2** below.

Table 2. SRA values and their interpretation [30,31].

SRA value	Interpretation
$SRA>2$	Extremely humid
$1.9>SRA>1.5$	Moderately wet
$0.99>SRA>-0.99$	Near normal
$-1.0>SRA>-1.49$	Moderately dry
$-1.5>SRA>-1.99$	Severely dry
$SRA<-2$	Extremely dry

• **Coefficient of Variation (CV)**

This is used to assess the variability of annual and seasonal precipitation data, and a higher value of CV indicates greater variability in the time series precipitation data [31]. The CV was calculated according to the following formula:

$$CV = \frac{\sigma}{\mu} \times 100 \qquad (2)$$

where CV is the coefficient of variation, in %, μ is the average value of precipitation data over the period 1992–2022; σ is the standard deviation of precipitation data over the same period. Its interpretation is as follows [31]:

(1) The CV value<20% represents less variability,

(2) The value 20%≤CV≤30% represents moderate variability and

(3) The value CV>30% represents a high variability of precipitation in the catchment.

• **Moving average (MA)**

This is an empirical tool used to smooth out the ef-fect of temporary variations in the data [32]. In the study, the moving average used a three-year interval to better capture the variability.

2.3.2. Methods for Estimating Rainfall Erosivity

Rainfall erosivity represents the erosive potential of raindrops that cause soil erosion [33]. The research [34] select five estimators of rainfall erosion: total annual precipitation (P), Fournier index (FI), modified Fournier index (MFI), precipitation concentration index (PCI) and regression model for rainfall erosion analysis. Fournier index (F), precipitation concentration index (PCI) and Pearson's correlation were used in this study.

• **Precipitation Concentration Index**

The Precipitation Concentration Index (PCI) is a useful indicator for estimating the monthly heterogeneity of precipitation [35]. As a result, an uneven distribution of precipitation can lead to periods of excess rain or drought, making it difficult for plants and crops to grow [36].

The research [35] proposed the Precipitation Concentration Index (PCI), derived from the Employment Diversification Index [37] and defined as follows:

$$PCI_{annual} = 100 \times \frac{\sum_{i=1}^{12} P_i^2}{\left(\sum_{i=1}^{12} P_i\right)^2} \qquad (3)$$

Où, $i = 1,….,12$ is the month of January, February, etc.; p_i is the rainfall for the i-th month.

It is interpreted in **Table 3** below.

Table 3. PCI values and their interpretation [35,38].

PCI values	Interpretation
ICP<10	Uniform distribution of monthly rainfall over the year
10≤ICP<16	Moderate distribution of monthly rainfall over the year
16≤ICP<20	Irregular distribution of monthly rainfall over the year
ICP>20	Distributions showing the monthly variability of precipitation over the year

- **Fournier Index (1970)**

Rainfall aggressiveness for the period 1992–2022 is assessed using the Fournier Index (FI), which requires monthly rainfall data. The FI has been calculated as follows:

$$FI = \frac{P_{\max i}^2}{P_i} \tag{4}$$

where, $P_{\max i}$ is the highest mean monthly precipitation, and P is the mean annual precipitation, n is time period and for the study, $n = 2022-1992 = 30$ years. **Table 4** below shows the level of aggressiveness of the rain.

- **Arnoldus index (1978)**

This index takes into account the ratio between the square sum of the mean monthly rainfall of each month of the year and the mean annual rainfall [40]. It differs from Fournier's index in that it takes into account the monthly rainfall of all months of the year. In contrast, the Fournier index focuses only on the rainfall of the wettest month. The Fournier index therefore complements the Arnoldus index (1978). It gives a better idea of the degree of erodibility of rainfall in the catchment. Its mathematical formula is operationalised as follows [40]:

$$AI = \frac{\sum_{i=1}^{12} p_i^2}{P} \tag{5}$$

where, p: average monthly rainfall in mm, P: average annual rainfall in mm.

Table 5 below shows the erosion risk assessment scale.

Table 4. Scale for assessing the aggressiveness of rainfall [39].

Classes of erosivity	Soil Loss (t/ha/yr)	FI Value	Risk of erosion	Colour
C1	<5	0–20	Very low	
C2	5–12	21–40	Low	
C3	12–50	41–60	Moderate	
C4	50–100	61–80	High	
C5	100–200	81–100	Very high	
C6	>200	>100	Extremely high	

Table 5. Rainfall aggressiveness assessment scale [40].

Classes of erosivity	AI value	Risk of erosion
C1	<60	Very low
C2	60<90	Low
C3	90<120	Moderate
C4	120<160	High
C5	>160	Very high

2.3.3. Trend Analysis of Erosion Indices

For trend analysis, the nature of the data was first checked using normality and autocorrelation tests, and then the Mann-Kendall test was selected according to the nature of the data.

- **Normality test**

This test is important in determining the appropriate methods for describing trends in precipitation time series. In this study, the Shapiro-Wilk, Lilliefors and Anderson-Darling tests were used to detect trend in precipitation time series. The null hypothesis is that the precipitation time series are stationary:

- the first hypothesis (H0) assumes that the data fol-

low a normal distribution;
- the second alternative (Ha) states that the data do not follow a normal distribution.

Hypothesis H_0 must be rejected when p-value<0.05.

Table 6 below shows that, overall, the data do not follow a normal distribution. This situation therefore requires the use of non-parametric tests. The Mann-Kendall test was used in this study.

Table 6. Normality tests for PCI and FI time series.

Index	Shapiro-Wilk	Anderson-Darling	Lilliefors
PCI			
PCI-dadounin	0.060	0.045	0.160
PCI-toyande	0.856	0.719	0.837
PCI-sole	0.716	0.729	0.799
PCI-Sinikiere	0.08	0.045	0.03
PCI-Tambarga	0.065	0.02	0.019
PCI-kompienga	0.077	0.034	0.025
PCI-gossina	0.210	0.119	0.136
FI			
FI-dadounin	0.323	0.483	0.593
FI-toyande	0.679	0.607	0.350
FI-sole	0.001	0.014	0.124
FI-Sinikiere	0.068	0.088	0.13
FI-Tambarga	0.074	0.081	0.25
FI-kompienga	0.085	0.098	0.138
FI-gossina	<0.0001	0.005	0.106

Source: https://power.larc.nasa.gov/data-access-viewer/.

- **Durbin-Watson test for autocorrelation**

The Durbin-Watson (DW) test is frequently used to detect autocorrelation in time series [39]. The hypothesis for this test is as follows [41,42]:

H_0: There data has no autocorrelation.

H_1: There data has autocorrelation.

The formula is:

$$d = \frac{\Sigma_{t=2}^{t=n}(e_t - e_{t-1})^2}{\Sigma_{t=1}^{n} e_t^2} \qquad (6)$$

The H_0 hypothesis must be rejected when p-value<0.05.

Table 7 below shows that all the PCI and FI time data are significantly auto-correlated.

Table 7. Autocorrelation tests for PCI and FI data.

Variable	DW	p-value
PCI		
PCI-Dadounin	0.017	<0.0001
PCI-Toyande	0.013	<0.0001
PCI-Sole	0.02	<0.0001
PCI-Sinikiere	0.04	<0.0105

Table 7. *Cont.*

Variable	DW	*p*-value
PCI-Tambarga	0.052	<0.005
PCI-Kompienga	0.14	<0.0001
PCI-Gossina	0.027	<0.0001
FI		
FI-Dadounin	0.175	<0.0001
FI-Toyande	0.1743	<0.0001
FI-Sole	0.379	<0.0001
FI-Sinikiere	0.425	<0.005
FI-Tambarga	0.3036	<0.002
FI-Kompienga	0.202	<0.0001
FI-Gossina	0.271	<0.0001

Source: https://power.larc.nasa.gov/data-access-viewer/.

• **Mann-Kendall and modified Mann-Kendall Test**

The MK trend test is one of the most popular and widely used trend detection methods [41]. The MK test for a time series $P_1, P_2, P_3 \ldots P_n$ of length n is given as [43,44]:

$$S = \sum_{j=1}^{n-1} \sum_{k=j+1}^{n} \text{sgn}(P_k - P_j) \qquad (7)$$

$$\text{sgn}(P_k - P_j) = \begin{cases} 1, \text{ if } P_k > P_j \\ 0, \text{ if } P_k = P_j \\ -1, \text{ if } P_k < P_j \end{cases} \qquad (8)$$

where, sgn(P_k–P_j) enotes the signum function of P and P_j. P_j and Pk are the rainfall values at time j and k for $j<k$. The j, k the value of S is generally positive when trend is increasing and negative when trend is decreasing. The variance of the MK statistic is given as:

$$var(s) = \frac{n(n-1)(2n+5) - \sum_{m=1}^{q} t_m(t_m-1)(2t_m+5)}{18} \qquad (9)$$

where q is the number of tied group and t_m is the total data values in m^{th} group.

The Z value is calculated after the calculation of the variance of time series data by following formula:

$$\begin{cases} \dfrac{S-1}{\sqrt{var(s)}}, \text{ if } S > 0 \\ 0, \text{ if } S = 0 \\ \dfrac{S+1}{\sqrt{var(s)}}, \text{ if } S < 0 \end{cases} \qquad (10)$$

This test involves testing the null hypothesis, H_0, of no trend against the alternative hypothesis, H_A, of an upward or downward trend, depending on the 5% *p*-value.

The presence of serial correlation or autocorrelation in hydrometeorological time series amplifies the rejection of the null hypothesis in the Mann-Kendall (Mk) test [45–47]. It is therefore important to take this into account (see **Table 7**).

Thus, some authors advocate pre-whitening, which consists of removing the effect of serial correlation from the data series before applying the Mann-Kendall test [48–51].

The methods for modifying the original Mann-Kendall trend tests are characterised by two levels (Hu et al., 2023): in the first level, autocorrelation is estimated and removed before the trend test, and in the other method, the distribution of the statistic due to persistence is modified.

In this study, the first method is considered, which incorporates a variance correction approach proposed by [46] to minimise autocorrelation effects, thereby increasing the reliability of trend detection. The research [46] proposed the modified variance of S statistics as follows [52]:

$$var(S)^* = var(S) \frac{n}{n^*} \qquad (11)$$

$$n^* = \frac{n}{1 + \dfrac{\rho_1^{n+1} - n^* \rho_1^2 + (n-1)^* \rho_1}{n^*(\rho_1 - 1)^2}} \qquad (12)$$

where n^* is the effective sample size, ρ_1 is the lag-1 auto-correlation coefficient, which is calculated for the detrended series. The XLSTAT 2018 spreadsheet incorporating the [52] method was used to process the data.

2.3.4. Pearson's Correlation

The correlation coefficient is used to assess the strength of the relationship between two or more variables that are statistically linked. It measures the strength and direction of the relationship between two variables [51]. The intensity reflects the strength or nature of the association between two variables. The closer the extremes of the interval (–1 and +1), the stronger the correlation. Pearson correlation measures the association between two variables (FI and PCI). **Table 8** below shows a classification of the Pearson correlation coefficient. In this study, Pearson correlation was used to measure the relationship between Fournier index (1970) and precipitation concentration index. Mathematically, it is expressed as follows:

$$r = \frac{\sum_{i=1}^{n} (x_i - \bar{x}) - (y_i - \bar{y})}{\sqrt{\sum (x_i - \overline{X})^2 (y_i - \overline{Y})^2}} \tag{13}$$

In the expression, $\overline{X}$ refers to the independent variables, while $\overline{Y}$ represents the independent variables.

The terms x_i and y_i refer to the values of the i-th observation in the variables $\overline{X}$ and $\overline{Y}$, respectively.

Table 8. Classification of Pearson's correlation [53].

Value	Interpretation
0	Null
0.10 a 0.30	Weak
0.40 a 0.6	Moderate
0.70 a 0.90	Strong
1	Perfect

3. Results

3.1. Characterization of Rainfall in the Nakambè Catchment Area

3.1.1. Seasonal Precipitation Variability is Moderate to High Over the 1992–2022 Period

The variability is excessive during the rainy pre-season and very high during the post-season. This could be explained by the erratic nature of rainfall during these periods. In addition, moderate variability is observed in June, July and August and high variability in September. This moderate variability could be explained by the fact that these months, in this case June, July and August, are the periods when monsoon winds are present throughout the region. In September, however, the monsoon winds begin to move out of the country. This means that rainfall becomes less regular throughout the country. In addition, rainfall is highly variable in the period following the rainy season. **Table 9** below summarises the variability of rainfall in the catchment area.

Table 9. Seasonal variability of rainfall in the catchment from 1992 to 2022.

Seasonality	Month	Dadounin	Gossina	Kompienga	Tambarga	Sinikiere	Sole	Toyandé
	JAN	310.56%	310.56%	373.87%	534.19%	556.78%	556.78%	556.78%
	FEB	252.76%	252.76%	204.80%	297.54%	281.64%	538.45%	549.25%
Rainy pre-season	MAR	127.99%	127.99%	156.20%	191.21%	226.82%	282.23%	389.62%
	APR	59.38%	59.38%	50.55%	76.81%	61.92%	174.76%	152.51%
	MAY	37.22%	37.22%	27.80%	36.27%	57.33%	140.40%	135.33%

Table 9. *Cont.*

Seasonality	Month	Dadounin	Gossina	Kompienga	Tambarga	Sinikiere	Sole	Toyandé
Season rainy	JUN	28.41%	28.41%	28.84%	30.35%	28.78%	41.96%	37.71%
	JUL	25.72%	25.72%	18%	19.01%	29.21%	28.57%	27.71%
	AUG	23.90%	23.90%	20.72%	22%	24.79%	33.69%	26.51%
	SEP	34.85%	34.85%	27.43%	27.58%	36.29%	35.32%	35.14%
Rainy post-season	OCT	92.03%	92.03%	52.68%	62.71%	72.86%	96.29%	98.97%
	NOV	242.04%	242.04%	253.83%	351.10%	346.60%	556.78%	519.43%
	DEC	404.67%	404.67%	212.12%	312.56%	556.78%	514.58%	489.62%

Source : https://power.larc.nasa.gov/data-access-viewer/.

3.1.2. Annual Rainfall Variability through the Normalised Rainfall Anomaly

An analysis of **Figure 2** shows that the Nakambè catchment has alternating dry and wet periods. However, the evolution of this phase depends on the climatic range of the basin. There are four climatic domains: the Sahelian zone (annual rainfall of less than 600 mm), the Sudano-Sahelian zone (annual rainfall between 600 and 900 mm), the Sahelo-Sudanian zone (annual rainfall of 900 mm or more) and the Sudanian zone (annual rainfall of 900 mm or more).

At stations such as Tambarga and Kompienga in the Sudanese zone, there are four phases: a wet phase from 1993 to 1999, followed by a dry phase from 2000 to 2003, then an alternating wet-dry phase from 2004 to 2017, and finally a wet phase from 2018 to 2022. In the Sudano-Sahelian zone, which includes the Dadounin, Gossina and Sinikiere stations, two phases are generally observed: a dry phase from 1992 to 2009 and a wet phase from 2010 to 2022. In the Sahelian zone, two phases are always observed, but with an increase in dry periods from 1992 to 2012, followed by a wet phase from 2013 to 2022.
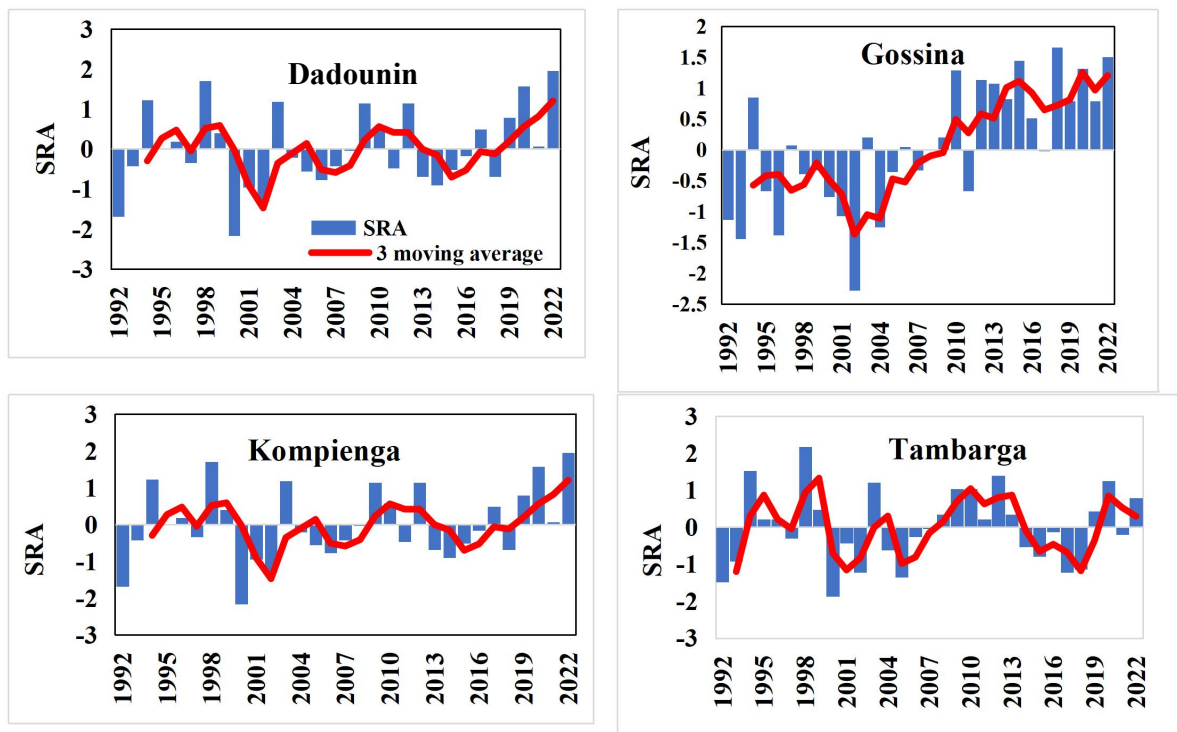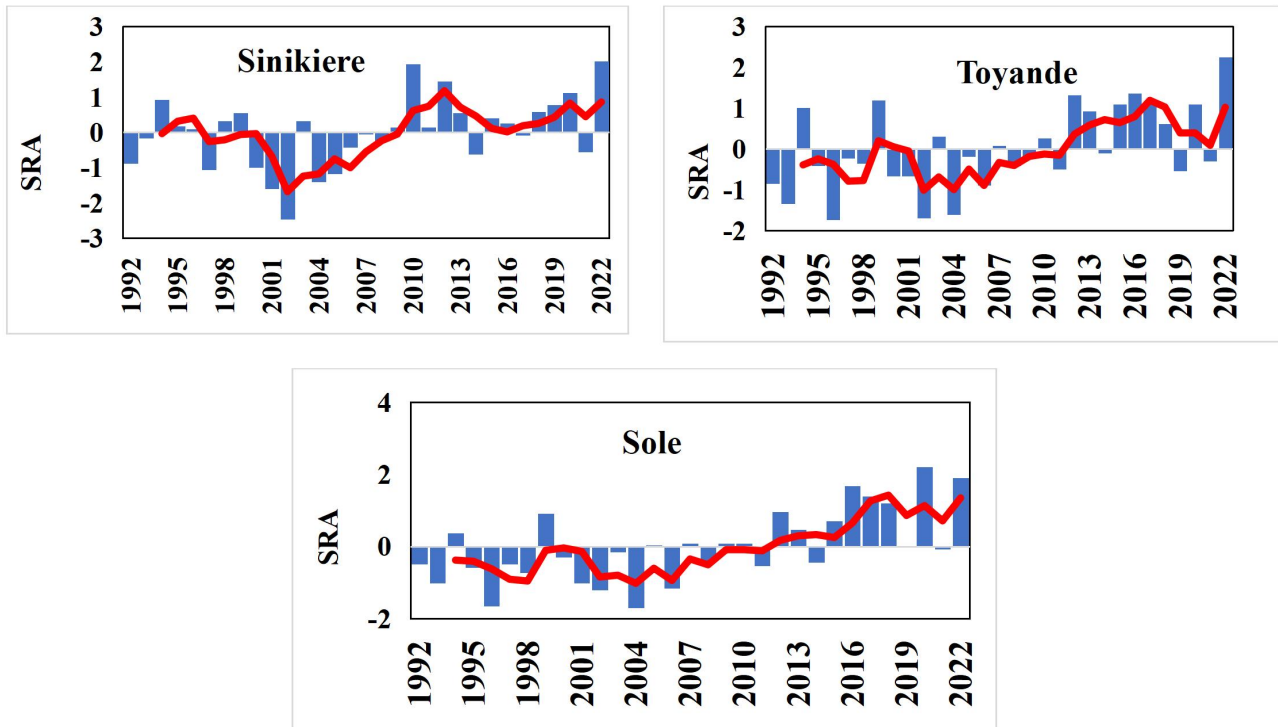

Figure 2. *Cont.*

Figure 2. Variability of rainfall anomalies in the catchment from 1992 to 2022.

3.2. Characterization of Rainfall Erosion in the Nakambè Watershed

Three indices were used to assess the level of rainfall erosivity over the period 1992–2022. These are the Fournier index (FI), the Arnoldus index (AI) and PCI.

3.2.1. Rainfall Erosion according to the Fournier Index (1970): between Variability and Upward Trend Over the Period 1992–2022

FI has shown that the level of rainfall erosion varies across the catchment (**Figure 3**).

Analysis of **Figure 3** shows that the FI fluctuates from year to year over the period 1992–2022. In addition, 57.14% of stations show an upward trend and 42.85% no trend at all (**Table 10**).

The table shows an upward trend at four of the seven stations. This situation could be explained by climatic conditions. Most of the stations with an upward trend in FI are located in the Sudano-Sahelian and Sahelian zones. Conversely, the stations with no trend are in the Sudanian domain. This would mean that August rainfall was on the increase in the Sudano-Sahelian and Sahelian domains, unlike the Sudanian domain through which the Nakambè catchment passes.
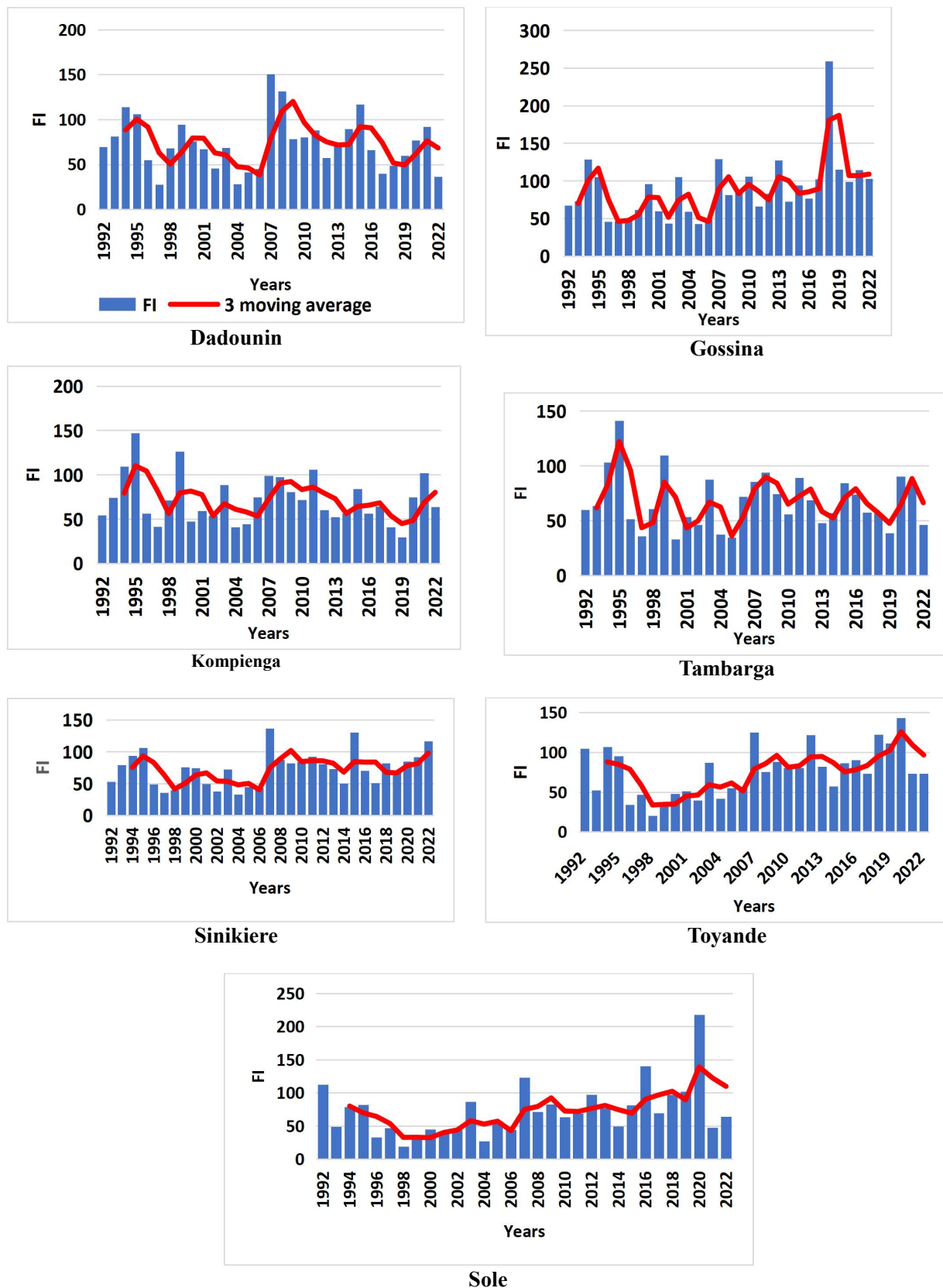
Figure 3. Variability and trend in the Fournier index (1970) over the period 1992–2022.

Table 10. Annual trend in erosivity in the catchment over the period 1992–2022.

Stations	Fournier index (1970)	Kendall's Tau	*p*-value	Trend	
Tambarga	FI-Tambarga	–0.019	0.685	No	-
Dadounin	FI-Dadounin	–0.062	0.247	No	-
Toyande	FI-Toyande	0.320	<0.0001	Yes	+
Sinikiere	FI-Sinikiere	0.204	<0.001	Yes	+
Sole	FI-Sole	0.286	<0.0001	Yes	+
Kompienga	FI-Kompienga	–0.075	0.089	No	-
Gossina	FI-Gossina	0.312	<0.0001	Yes	+

Source: https://power.larc.nasa.gov/data-access-viewer/

3.2.2. Monthly Trend in Rainfall Erosivity according to the Arnoldus Index (1978)

The Arnoldus index shows that rainfall erosion occurs during the rainy period. However, the month of August has the highest occurrence of rain erosion. This erosion was moderate from 1992 to 2000, and high from 2001 to 2022. Areas of the catchment located in the Sudano-Sahelian and Sahelian domains are more affected by rain erosion. **Figure 4** illustrates this situation. In this figure, blue indicates low erosion, dark and light-yellow moderate erosion, and red high and very high erosion.

3.3. Variability and Trends of Precipitation Concentrations at the Catchment Scale

Rainfall concentration is a function of the climatic zones of the watershed. Variability in rainfall concentration is high at stations such as Dadounin, Gossina and Kompienga, which are located in the Sudano-Sahelian and Sudanian zones. In addition, concentrations are low to moderate. This means that rainfall homogeneity during the rainy season is unbalanced. Rainfall is more or less evenly distributed over the months of June, July, August and September. By contrast, in the Sahelian zone, to which the Sole and Toyande stations belong, rainfall variation is low. However, rainfall concentrations are high (PCI≥20).

This means that the rainfall distribution during the rainy season is irregular and concentrated in three months: July, August and September. **Figure 5** summarizes the rainfall concentrations for stations that do not have similar data. Some stations have not been taken into account, notably Tambarga and Sinikiere, because they have the same characteristics as the Kompienga and Gossina stations. This is due to the climate. The Kompienga and Tambarga stations are located in the Sudanian domain, and the Sinikiere and Gossina stations are located in the Sudano-Sahelian domain.

Table 11 below shows that stations in the Sudano-Sahelian and Sahelian domains show upward trends. No trend was reported for the station located in the Sudanian domain.
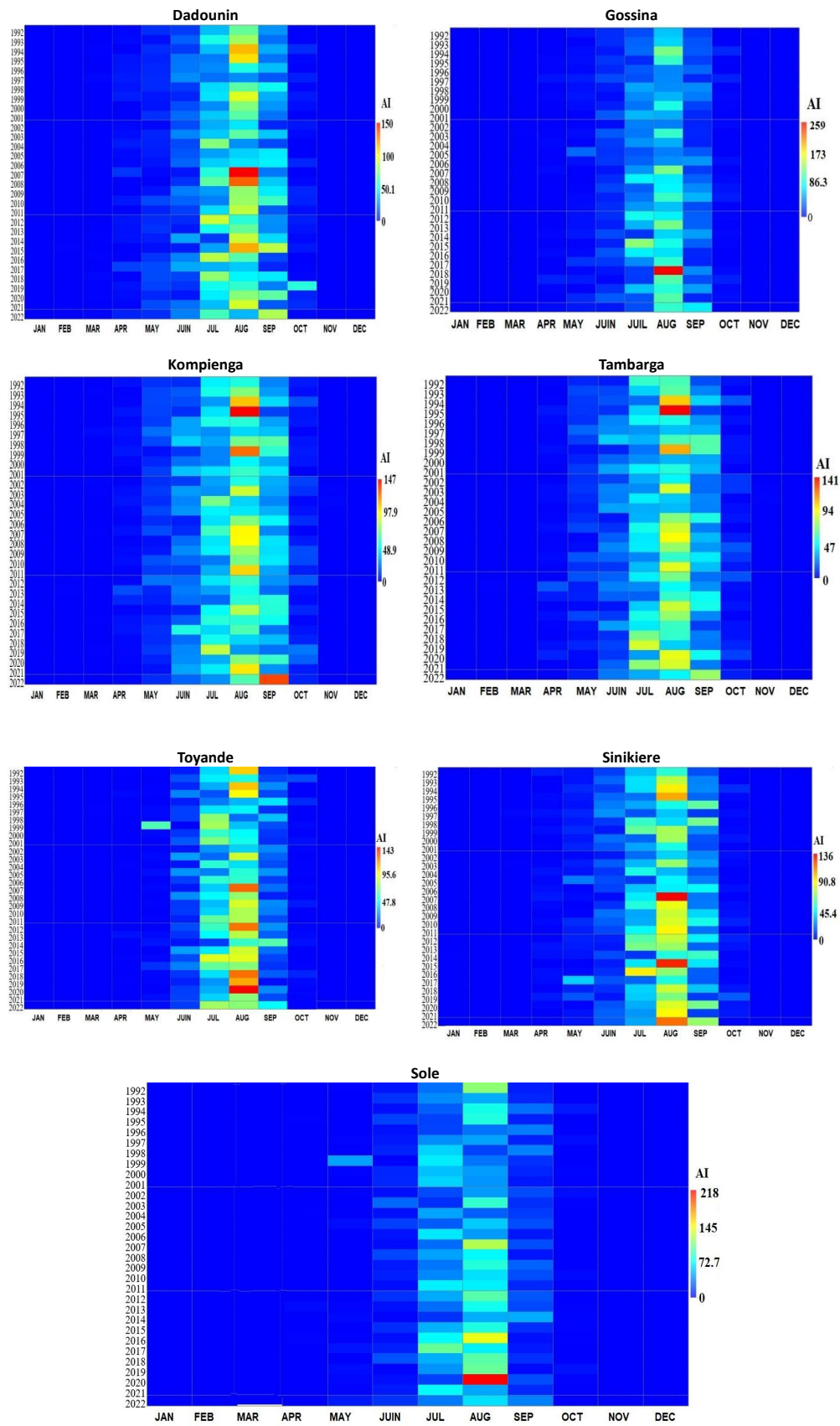
Figure 4. Monthly trends in rainfall erosion in the watershed over the period 1992–2022.
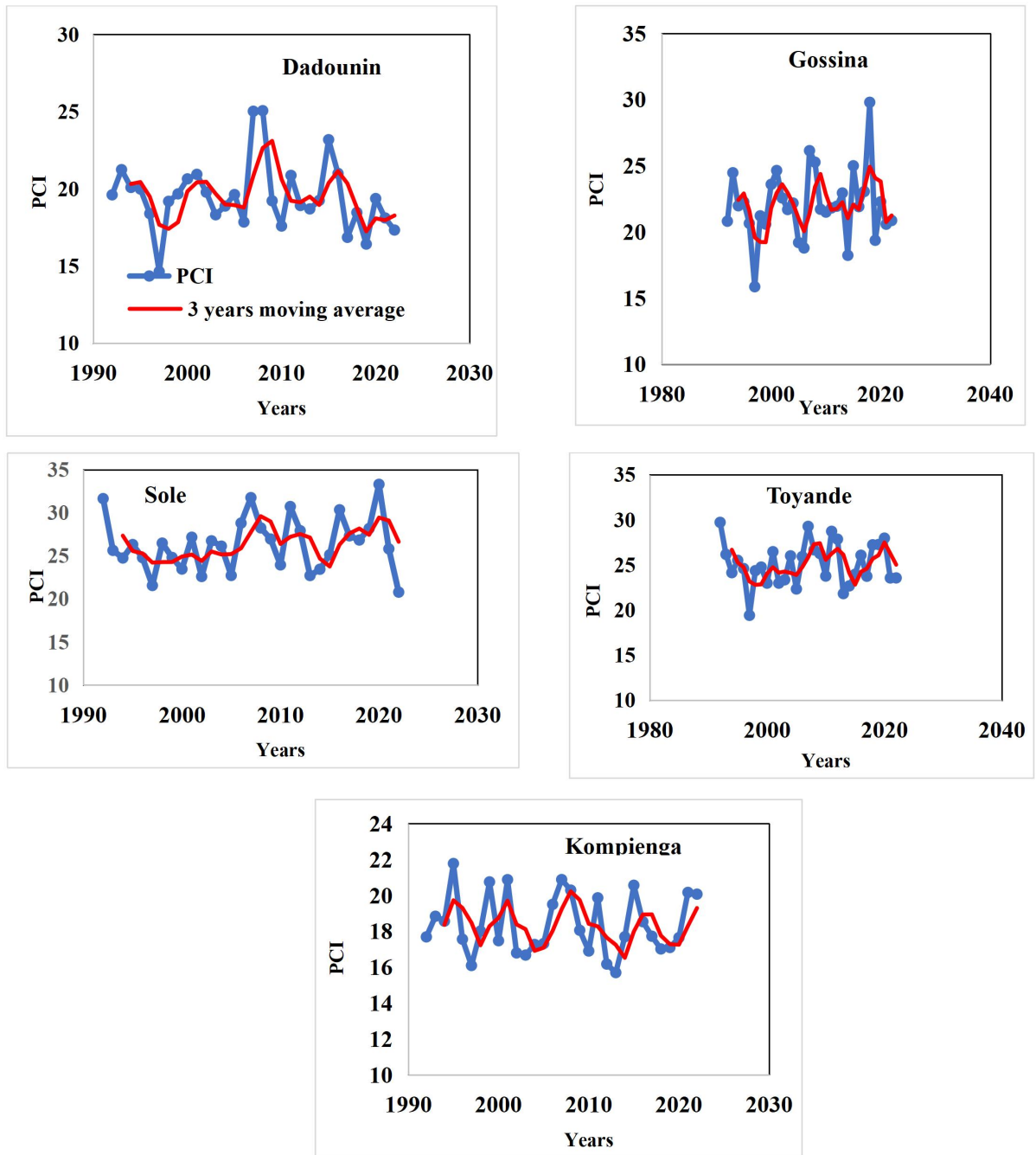
Figure 5. Variability of precipitation concentrations at watershed scale.

Table 11. Trends in precipitation concentration indices from 1992 to 2022.

Stations	PCI	Kendall's Tau	*p*-value	Trend	
Dadounin	PCI-Dadounin	-0.204	<0.0001	Yes	+
Toyande	PCI-Toyande	0.037	0.473	No	-
Sole	PCI-Sole	0.118	0.007	Yes	+
Sinikiere	PCI-Sinikiere	0.111	0.002	Yes	+
Tambarga	PCI-Tambarga	0.115	0.009	Yes	+

Table 11. *Cont.*

Stations	PCI	Kendall's Tau	*p*-value	Trend	
Kompienga	PCI-Kompienga	-0.041	0.305	No	-
Gossina	PCI-Gossina	0.041	0.368	No	-

Source: https://power.larc.nasa.gov/data-access-viewer/.

3.4. Relationship between Rainfall Erosion, Precipitation Concentration Index, and Standardized Precipitation Anomaly

The ability of raindrops to cause erosion depends on three factors: the intensity, frequency and duration of the precipitation. When precipitation is concentrated over a short period of time, a large amount of water falls on the soil, inevitably leading to severe erosion (**Table 12**).

Table 12 shows the relationship between FI and PCI. It is highly significant at the Dadounin, Gossina, Sinikiere, Tambarga and Kompienga stations and significant at the Sole, Gossina and Toyande stations. In addition, rainfall variability leads to different trends in rain erosion (**Table 13**).

Table 13 shows the significance of the relationships between SRA and FI over the period 1992–2022. However, the relationships are stronger when the station is in the Sahelian domain, such as Sole with r:0.642, and stations in the Sudano-Sahelian domain, such as Gossina and Sinikiere, with correlation coefficients of r:0.59 and r:0.562 respectively. It should be noted that the correlation in the Sudanese domain is weak. Thus, over the extent of the Nakambè catchment, rainfall variability has a greater impact on rainfall erosion in the Sahelian and Sudano-Sahelian zones of the basin.

Table 12. Degree of influence of PCI on FI over the period 1992–2022.

Stations	Correlation coefficient	*p*-Value	Relationship
Dadounin	0.764	0.000	Very significant
Toyande	0.547	0.001	Significant
Sole	0.654	0.000	Significant
Kompienga	0.713	0.000	Very significant
Gossina	0.710	0.000	Very significant
Sinikiere	0.709	0.000	Very significant
Tambarga	0.712	0.000	Very significant

Source: https://power.larc.nasa.gov/data-access-viewer/.

Table 13. Level of influence between the SRA and the FI.

Stations	Correlation coefficient	*p*-Value	Relationship
Dadounin	0.225	0.223	No significant
Toyande	0.473	0.007	Significant
Sole	0.642	0.000	Significant
Kompienga	0.242	0.191	Very significant
Gossina	0.59	0.001	Very Significant
Sinikiere	0.562	0.001	Very Significant
Tambarga	0.388	0.031	Significant

Source: https://power.larc.nasa.gov/data-access-viewer/.

4. Discussion

4.1. Recent Rainfall Variability and Trends in the Watersheds of Burkina Faso

The Nakambè watershed is characterised by high variability, punctuated by alternations between dry and wet periods, depending on the climatic zones crossed by the watershed. These trends are similar to those observed in other studies of the watershed in Burkina Faso. The researches [18,54] also observed the same rainfall variability over the period 1988–2018. This trend and variability are expected to continue until 20250 [55]. Other studies on several watersheds in Burkina Faso show similar results. In the Sourou watershed, the research [56] found interannual variability characterised by dry phases (1971–1993) and wet phases (1994–2009). The same trends were also observed in the Inner Mouhoun watershed over the period 1970–2010 [57] and in the Nakambè-Mané watershed between 1991 and 2020 [58]. The wet phases observed in the different basins of Burkina Faso lead to a significant increase in flooding in the Kou basin [59] and in the Sourou basin [60]. In West Africa, the same trends have been observed by several authors. Indeed, the research [61] in the Mono River watershed (Benin, Togo) shows that rainfall has been highly variable over the period 1981–2010, and by 2050, the two scenarios predict a very sharp increase in variability. This situation should lead to a change in the seasonal rainfall cycle in the catchment. Other studies, notably [62], have revealed a moderate risk of erosion during the long rainy season (April to July), a low risk of erosion during the short rainy season (August to October) and a very low risk of erosion during the dry season (November to March). This is somewhat different from the results of the study, which show that the risk of rain erosion is very high during the month of August. This situation could be explained by the fact that rainfall in Burkina Faso is characterized by an increase in extreme precipitation, which leads to heavy flooding during this month, thus increasing the risk of rain erosion.

4.2. Rainfall Erosion: Rainfall is the Main Factor in Soil Erosion

The study of the Nakambè catchment shows that rainfall erosion is variable and has an upward trend over the period 1992–2022. August, the wettest month, influences the level of rainfall erosion in the Nakambè catchment. The correlation between the rainfall concentration index, SRA, and the Fournier index shows that there is a close relationship between rainfall concentration and the level of rainfall erosion. Furthermore, the variable nature of rain erosion is strongly influenced by the SRA. Studies from around the world confirm the results of the study. The results of the study are confirmed by work in West Africa. In fact, in the Lower Niger Basin, the research [63] indicate an increasing trend in the erosivity of annual rainfall runoff, with an average change in rainfall runoff erosivity of about 14.1%, 19% and 24.2% for the years 2030, 2050 and 2070 respectively. This situation can be attributed to the change in precipitation characteristics in West Africa, with the occurrence of extreme precipitation events leading to an increase and variation in rainfall erosion [64]. Similar results have been observed in eastern and southern Africa. Indeed, the research [65] in Kenya also found an increase in rain erosion with a land loss of 4.76 t ha-1 yr-1. The researches [66–68] found that rain erosion varies from month to month and from year to year. The research [69] adds that the Armoldus Index (1978) shows a strong trend over Burkina Faso between 2000 and 2023. In the Loess Plateau of China, the research [70] also found a linear relationship between mean rainfall and erosivity. The authors found that the Fournier index increases with rainfall. In Algeria, the Tango-Arnoldus index of Arnoldus (1980) evolves as a function of annual rainfall in the Macta catchment [71]. Several other studies, in the Himalayan basin of India [72], in Turkey [73]. In southern Portugal, there is a general trend towards an increase in the amount, concentration and erosivity of rainfall in autumn and summer, suggesting an increase in the potential risk of soil erosion [74]. Conversely, the work [75] in other European countries presents different results on the occurrence of rain erosion risk induced by increased precipitation. In fact, the authors note a sudden increase in rain erosion in most of the European Union in May and the highest values are recorded during the summer months, a less rainy period according to the European countries.

5. Conclusions

Climate change is causing changes in rainfall pat-

terns. This leads to variations in rainfall erosivity over time. It is important to understand the temporal trends in rainfall, runoff and erosivity, and the factors that influence rainfall erosion. This study examines rainfall and erosion trends, as well as variability, in the Nakambè catchment. The coefficient of variation and the standardised rainfall index revealed high variability, particularly over the last decade, during which there have been periods of heavy rainfall. This affects the erosivity of rainfall in the basin. The Fournier index, the Arnoldus index and the rainfall concentration index therefore indicate the presence of rain erosion in the catchment between 1992 and 2022. Rain erosion is strongest during rainy periods and weakest during the dry season. Consequently, land loss occurs during the rainy season, particularly in August. The area has more than a hundred dams, which are very important for the economy and for people's lives. So, it is very important that the people in charge and the local people work together to stop the problem of rainwater erosion. To this end, farmers around the catchment area should implement soil conservation techniques. Additionally, local authorities should implement reforestation programs in the catchment area to reduce water runoff and slow down land loss caused by rainwater erosion.

Author Contributions

Research ideas, J.Y. and S.R.; conceptualization, J.Y.; data acquisition, J.Y.; statistical analysis of data, J.Y., S.R. and S.K.; methodology, J.Y., S.R. and S.K.; manuscript writing, J.Y.; manuscript proofreading, S.R.; participating in data processing, R.Z. All authors have read and agreed to the published version of the manuscript.

Funding

This work received no external funding.

Institutional Review Board Statement

Not applicable.

Informed Consent Statement

Not applicable.

Data Availability Statement

The datasets generated by this study are available from: https://power.larc.nasa.gov/data-access-viewer/.

Acknowledgments

Conflicts of Interest

The authors declare no conflict of interest.

References

[1] Zhang, Q., Berntell, E., Li, Q., et al., 2021. Understanding the variability of the rainfall dipole in West Africa using the EC-Earth last millennium simulation. Climate Dynamics. 57(1), 93–107. DOI: https://doi.org/10.1007/s00382-021-05696-x

[2] Nicholson, S.E., 2013. The West African Sahel: A review of recent studies on the rainfall regime and its interannual variability. International Scholarly Research Notices. 2013(1), 453521. DOI: https://doi.org/10.1155/2013/453521

[3] Ibrahim, B., Nazoumou, Y., Fowe, T., et al., 2021. Identification of a Representative Stationary Period for Rainfall Variability Description in the Sudano-Sahelian Zone of West Africa during the 1901–2018 Period. Atmosphere. 12(6), 716. DOI: https://doi.org/10.3390/atmos12060716

[4] Agbo, E.P., Offorson, G.C., Yusuf, A.S., et al., 2025. Innovative trend analysis of precipitation changes over Nigeria: A case study of locations across the Niger and Benue Rivers. Journal of the Nigerian Society of Physical Sciences. 7(1), 1868. DOI: https://doi.org/10.46481/jnsps.2025.1868

[5] Larbi, I., Nyamekye, C., Hountondji, F.C., et al., 2020. Climate change impact on climate extremes and adaptation strategies in the Vea catchment, Ghana. In: Leal Filho, W., Oguge, N., Ayal, D., Adeleke, L., da Silva, I. (eds.). African Handbook of Climate Change Adaptation. Springer Nature: Cham, Switzerland. pp. 1–17.

[6] Nyatuame, M., Agodzo, S.K., Amekudzi, L.K., 2022. Analysis of rainfall and temperature trend and variability of the Tordzie Watershed. Ghana Journal of Science, Technology and Development. 8(1), 1–17. DOI: https://doi.org/10.47881/271.967x

[7] Noba, W.G., Damiba, L., Doumounia A., et al., 2024. Climate projection and future rainfall trends

analysis in the Nouhao sub-basin in Burkina Faso. Global NEST Journal. 26(3), 1–10. DOI: https://doi.org/10.30955/gnj.005724

[8] Yaméogo, J., Sawadogo, A., 2024. Consequences of precipitation variability and socio-economic activity on surface water in the Vranso water basin (Burkina Faso). Glasnik Srpskog Geografskog Drustva. 104(1), 255–266. DOI: https://doi.org/10.2298/gsgd2401255y

[9] Yao, B.A.F., Soro, G.E., Larbi, I., et al., 2024. Effects of climate variability and/or land use dynamics on the hydrological balance of the Cavally River catchment at Toulepleu, West Africa. Journal of Water and Climate Change. 15(5), 2092–2109. DOI: https://doi.org/10.2166/wcc.2024.512

[10] Coulibaly, N., Coulibaly, T.J.H., Mpakama, Z., et al., 2018. The impact of climate change on water resource availability in a trans-boundary basin in West Africa: The case of Sassandra. Hydrology. 5(1), 12. DOI: https://doi.org/10.3390/hydrology5010012

[11] Ebodé, V.B., Mahé, G., Amoussou, E., 2021. Impact de la variabilité climatique et de l'anthropisation sur les écoulements de la Bénoué (nord Cameroun) [Impact of climatic variability and human activity on runoff from the Benoué (northern Cameroon)]. Proceedings of the International Association of Hydrological Sciences. 384, 261–267. DOI: https://doi.org/10.5194/piahs-384-261-2021 (in French)

[12] Markantonis, V., Farinosi, F., Dondeynaz, C., et al., 2018. Assessing floods and droughts in the Mékrou River basin (West Africa): a combined household survey and climatic trends analysis approach. Natural Hazards and Earth System Sciences. 18, 1279–1296. DOI: https://doi.org/10.5194/nhess-18-1279-2018

[13] Yéo, W.E., Goula, B.T.A., Diekkrüger, B., et al., 2016. Vulnerability and adaptation to climate change in the Comoe River Basin (West Africa). SpringerPlus. 5(1), 1–15. DOI: https://doi.org/10.1186/s40064-016-2491-z

[14] Angulo-Martínez, M., Beguería, S., 2009. Estimating rainfall erosivity from daily precipitation records: A comparison among methods using data from the Ebro Basin (NE Spain). Journal of hydrology. 379(1–2), 111–121. DOI: https://doi.org/10.1016/j.jhydrol.2009.09.051

[15] Diouf, R.N., Faye, C., Dieye, S., et al., 2021. in Distribution spatiale et tendances temporelles de l'érosivité des précipitations dans des bassins versants du sud du Sénégal (Gambie et Casamance)[Spatial distribution and temporal trends in rainfall erosivity in catchment areas of southern Senegal (Gambia and Casamance)]. Liens, Revue Internationale des Sciences et Technologies de l'Éducation. 1(1), 361–379. DOI: https://doi.org/10.1999/ve2t0p09 (in French)

[16] Gbohoui, Y.P., Paturel, J.E., Tazen, F., et al., 2021. Impacts of climate and environmental changes on water resources: A multi-scale study based on Nakanbé nested watersheds in West African Sahel. Journal of Hydrology: Regional Studies. 35, 100828. DOI: https://doi.org/10.1016/j.ejrh.2021.100828

[17] Zouré, C.O., Kiema, A., Yonaba, R., et al., 2023. Unravelling the Impacts of Climate Variability on Surface Runoff in the Mouhoun River Catchment (West Africa). Land. 12(11), 2017. DOI: https://doi.org/10.3390/land12112017

[18] Koala, S., Nakoulma, G., Dipama, J.-M., 2022. in Évolution Des Précipitations Et De La Température À l'Horizon 2050 Avec Les Modèles Climatiques CMIP5 Dans Le Bassin Versant Du Nakambé (Burkina Faso)[Changes in Precipitation and Temperature to 2050 Using CMIP5 Climate Models in the Nakambé Watershed (Burkina Faso)]. International Journal of Progressive Sciences and Technologies (IJPSAT). 37(2), 110–124. DOI: https://doi.org/10.52155/ijpsat.v37.2.5133 (in French)

[19] Tan, M.L., Armanuos, A.M., Ahmadianfar, I., et al., 2023. Evaluation of NASA POWER and ERA5-Land for estimating tropical precipitation and temperature extremes. Journal of Hydrology. 624, 129940. DOI: https://doi.org/10.1016/j.jhydrol.2023.129940

[20] Al-Kilani, M.R., Rahbeh, M., Al-Bakri, J., et al., 2021. Evaluation of remotely sensed precipitation estimates from the NASA POWER project for drought detection over Jordan. Earth Systems and Environment. 5(3), 561–573. DOI: https://doi.org/10.1007/s41748-021-00245-2

[21] Yaméogo, J., 2024. Changes in the seasonal cycles of extreme temperatures in the Sudano-Sahelian domain in West Africa: a case study from Burkina Faso. Meteorology Hydrology and Water Management. 12(2). DOI: https://doi.org/10.26491/mhwm/194451

[22] Okafor, G.C., Larbi, I., Chukwuma, E.C., et al., 2021. Local climate change signals and changes in climate extremes in a typical Sahel catchment: The case of Dano catchment, Burkina Faso. Environmental Challenges. 5, 100285, DOI: https://doi.org/10.1016/j.envc.2021.100285

[23] Kwawuvi, D., Mama, D., Agodzo, S.K., et al., 2022. An investigation into the future changes in rainfall onset, cessation and length of rainy season in the Oti River Basin, West Africa. Modeling Earth Systems and Environment. 8, 5077–5095. DOI: https://doi.org/10.1007/s40808-022-01410-w

[24] Ndiaye, P.M., Bodian, A., Diop, L., et al., 2021. Future trend and sensitivity analysis of evapotranspiration in the Senegal River Basin. Journal of Hydrology: Regional Studies. 35, 100820. DOI: https://doi.org/10.1016/j.ejrh.2021.100820

[25] Alemayehu, A., Maru, M., Bewket, W., et al., 2020. Spatiotemporal variability and trends in rainfall and

temperature in Alwero watershed, western Ethiopia. Environmental Systems Research. 9(1), 1–15. DOI: https://doi.org/10.1186/s40068-020-00184-3

[26] Harka, A.E., Jilo, N.B., Behulu, F., 2021. Spatial-temporal rainfall trend and variability assessment in the Upper Wabe Shebelle River Basin, Ethiopia: Application of innovative trend analysis method. Journal of Hydrology: Regional Studies. 37, 100915. DOI: https://doi.org/10.1016/j.ejrh.2021.100915

[27] De, A., Shreya, S., Sarkar, N., et al., 2023. Time series trend analysis of rainfall and temperature over Kolkata and surrounding region. Atmósfera. 37, 71–84. DOI: https://doi.org/10.20937/atm.53059

[28] Talib, S.A.A., Idris, W.M.R., Neng, L.J., et al., 2024. Irregularity and time series trend analysis of rainfall in Johor, Malaysia. Heliyon. 10(9), 1–18. DOI: https://doi.org/10.1016/j.heliyon.2024.e30324

[29] Taye, M., Mengistu, D., Sahlu, D., 2024. Characterizing the variability and trend of rainfall in central highlands of Abbay Basin, Ethiopia: using IMERG-06 dataset. European Journal of Remote Sensing. 57(1), 2372856. DOI: https://doi.org/10.1080/22797254.2024.2372856

[30] Shitu, K., Hymiro, A., Tesfaw, M., et al., 2024. Temporal rainfall variability and drought characterization in Cheleka Watershed, Awash River Basin, Ethiopia. Journal of Hydrology: Regional Studies. 51, 101663. DOI: https://doi.org/10.1016/j.ejrh.2024.101663

[31] Asfaw, A., Simane, B., Hassen, A., et al., 2018. Variability and time series trend analysis of rainfall and temperature in north central Ethiopia: a case study in Woleka sub-basin. Weather Clim Extremes. 19, 29–41. DOI: https://doi.org/10.1016/j.wace.2017.12.002

[32] Akrami, S.A., El-Shafie, A., Naseri, M., et al., 2014. Rainfall data analyzing using moving average (MA) model and wavelet multi-resolution intelligent model for noise evaluation to improve the forecasting accuracy. Neural Computing and Applications. 25, 1853–1861. DOI: https://doi.org/10.1007/s00521-014-1675-0

[33] Mello, C.D., Viola, M.R., Beskow, S., et al., 2013. Multivariate models for annual rainfall erosivity in Brazil. Geoderma. 202, 88–102. DOI: https://doi.org/10.1016/j.geoderma.2013.03.009

[34] Hernando, D., Romana, M.G., 2015. Estimating the rainfall erosivity factor from monthly precipitation data in the Madrid Region (Spain). Journal of Hydrology and Hydromechanics. 63(1), 55–62. DOI: https://doi.org/10.1515/johh-2015-0003

[35] Michiels, P., Gabriels, D., Hartmann, R., 1992. Using the seasonal and temporal precipitation concentration index for characterizing the monthly rainfall distribution in Spain. Catena. 19(1), 43–58. DOI: https://doi.org/10.1016/0341-8162(92)90016-5

[36] Kingbo, A., Teka, O., Aoudji, A.K.N., et al., 2022. Climate Change in Southeast Benin and Its Influences on the Spatio-Temporal Dynamic of Forests, Benin, West Africa. Forests. 13(5), 698. DOI: https://doi.org/10.3390/f13050698

[37] Gibbs, J.P., Martin, W.T., 1962. Urbanization, technology, and the division of labor: International patterns. American sociological review. 27(5), 667–677. DOI: https://doi.org/10.2307/2089624

[38] Oliver, J.E., 1980. Monthly precipitation distribution: a comparative index. The Professional Geographer. 32(3), 300–309. DOI: https://doi.org/10.1111/j.0033-0124.1980.00300.x

[39] Dumitraşcu, M., Dragotă, C.S., Grigorescu, I., et al., 2017. Key pluvial parameters in assessing rainfall erosivity in the south-west development region, Romania. Journal of Earth System Science. 126, 1–17. DOI: https://doi.org/10.1007/s12040-017-0834-y

[40] Maamar-Kouadri, K., Kouri, L., Chebouti, Y., 2016. in Utilisation de l'Indice d'Arnoldus pour cartographier les risques d'érosivité des pluies dans le Tell oranais (Algérie)[Use of the Arnoldus Index to map the risk of rainfall erosion in the Tell of Oran (Algeria)]. Geo-Eco-Trop. 40(4), 287–296.(in French)

[41] Turner, S.L., Forbes, A.B., Karahalios, A., et al., 2021. Evaluation of statistical methods used in the analysis of interrupted time series studies: a simulation study. BMC medical research methodology. 21, 1–18. DOI: https://doi.org/10.1186/s12874-021-01364-0

[42] Kumar, N.K., 2023. Autocorrelation and heteroscedasticity in regression analysis. Journal of Business and Social Sciences. 5(1), 9–20. DOI: https://doi.org/10.3126/jbss.v5i1.72442

[43] Yue, S., Pilon, P., Phinney, B., et al., 2002. The influence of autocorrelation on the ability to detect trend in hydrological series, Hydrol. Processes. 16, 1807–1829. DOI: https://doi.org/10.1002/hyp.1095

[44] Ranjan, S., Singh, L., Bahuguna, A., et al., 2023. Analysis of Trend Using Nonparametric Test for Rainfall and Rainy-Days in Jodhpur Zone of Rajasthan. Indian Journal of Ecology. 50(4), 1063–1068. DOI: https://doi.org/10.55362/IJE/2023/4014

[45] Yaméogo, J., 2025. Annual rainfall trends in the Burkina Faso Sahel: a comparative analysis between Mann–Kendall and innovative trend method (ITM). Discover Applied Sciences. 7, 221. DOI: https://doi.org/10.1007/s42452-025-06675-1

[46] Hamed, K.H., Rao, A.R., 1998. A modified Mann-Kendall trend test for autocorrelated data. Journal of hydrology. 204(1–4), 182–196. DOI: https://doi.org/10.1016/S0022-1694(97)00125-X

[47] Koutsoyiannis, D., 2003. Climate change, the Hurst phenomenon, and hydrologicalal statistics. Hydrologicalal Sciences Journal-Journal Des Sciences Hydrologiques. 48(1), 3–24. DOI: https://doi.

org/10.1623/hysj.48.1.3.43481

[48] Yue, S., Wang, C.Y., 2004. The Mann-Kendall test modified by effective sample size to detect trend in serially correlated hydrologicalal series. Water Resources Management. 18(3), 201–218. DOI: https://doi.org/10.1023/B: WARM.0000043140.61082.60

[49] Cammalleri, C., Sarwar, A.N., Avino, A., et al., 2024. Testing trends in gridded rainfall datasets at relevant hydrological scales: A comparative study with regional ground observations in Southern Italy. Journal of Hydrology: Regional Studies. 55(12), 101950. DOI: https://doi.org/10.1016/j.ejrh.2024.101950

[50] Bayazit, M., Önöz, B.J.H.S.J., 2007. To prewhiten or not to prewhiten in trend analysis? Hydrological Sciences Journal. 52(4), 611–624. DOI: https://doi.org/10.1623/hysj.52.4.611

[51] Kumar, M., Denis, D.M., Suryavanshi, S., 2016. Long-term climatic trend analysis of Giridih district, Jharkhand (India) using statistical approach. Modeling Earth Systems and Environment. 2, 116. DOI: https://doi.org/10.1007/s40808-016-0162-2

[52] Fathian, F., Dehghan, Z., Bazrkar, M.H., et al., 2016. Trends in hydrological and climatic variables affected by four variations of the Mann-Kendall approach in Urmia Lake basin, Iran. Hydrological Sciences Journal. 61(5), 892–904. DOI: https://doi.org/10.1080/02626667.2014.932911

[53] Dancey, C., Reidy, J., 2006. in Estatística sem matemática para psicologia: Usando SPSS para-Windows.[Statistics without maths for psychology: Using SPSS for Windows]. Artmed: Porto Alegre, Brazil, 608.(in French)

[54] Koala, S., Seydou, W., Dipama, J-M., 2023b. in Tendances pluviométriques récentes: vers une reprise de la pluviométrie au sahel. Cas du bassin versant du Nakambé (Burkina Faso)[Recent rainfall trends: towards an upturn in rainfall in the Sahel. The Nakambé catchment (Burkina Faso)]. pp.12-27 .(in French)

[55] Koala, S., Dipama, J.M., Vissin, E.W., 2023a. Evolution of Extreme Rainfall and Temperature Indices in the Nakambé Watershed at the Bagré Outflow (Burkina Faso). International Journal of Advanced Engineering and Management Research. 8(2), 154–169. DOI: https://doi.org/10.51505/ijaemr.2023.8214

[56] Karambiri, B.L.C.N., Dipama, J.M., Sanou, K., 2019. in Variabilité climatique et gestion efficiente de l'eau dans le bassin versant du Sourou au Burkina Faso[Climate variability and efficient water management in the Sourou catchment in Burkina Faso]. Revue de Géographie de l'Université de Ouagadougou. 8(1), 65–83.(in French)

[57] Kambire, G., Sirima, A.B., Rouamba, S., et al, 2023. in Variabilité hydro-climatique, aménagements hydrauliques et incidence sur le régime du fleuve Mouhoun a Dapola et Boromo[Hydro-climatic variability, hydraulic developments and impact on the regime of the Mouhoun River at Dapola and Boromo]. Collection recherches & regards d'Afrique. 3(3), 33–59.(in French)

[58] Yameogo, W.V.M., Kabore, O., Sanon, Z., et al., 2023.in Dynamique spatio-temporelle des surfaces en eau du bassin du Nakanbé-Mané au Burkina Faso[Spatial and temporal dynamics of water surfaces in the Nakanbé-Mané basin in Burkina Faso]. International Journal of Biological and Chemical Sciences. 17(1), 233–246. DOI: https://doi.org/10.4314/ijbcs.v17i1.17 (in French)

[59] Guelbeogo, S., Ouedraogo, L., Ilboudo, S., 2023. in Prévision des crues dans le bassin versant du Kou, Burkina Faso[Flood forecasting in the Kou catchment area, Burkina Faso]. International Journal of Biological and Chemical Sciences. 17(3), 1131–1146. DOI: https://dx.doi.org/10.4314/ijbcs.v17i3.29 (in French)

[60] Karambiri, B.L.C.N., 2023. in Les inondations d'octobre et de novembre 2022 dans la vallée du Sourou au Burkina Faso[The floods of October and November 2022 in the Sourou valley in Burkina Faso]. Collection Pluraxes monde. 44–64.(in French)

[61] Lawin, A.E., Hounguè, N.R., Biaou, C.A., et al., 2019. Statistical analysis of recent and future rainfall and temperature variability in the Mono River watershed (Benin, Togo). Climate. 7(1), 8. DOI: https://doi.org/10.3390/cli7010008

[62] Andoh, H.F., Antwi, B.O., Wakatsuiki, T., et al., 2012. Estimation of soil erodibility and rainfall erosivity patterns in the agroecological zones of Ghana. Journal of Soil Science and Environmental Management. 3(11), 275–279. DOI: https://doi.org/10.5897/JSSEM11.081

[63] Amanambu, A.C., Li, L., Egbinola, C.N., et al., 2019. Spatio-temporal variation in rainfall-runoff erosivity due to climate change in the Lower Niger Basin, West Africa. Catena. 172, 324–334. DOI: https://doi.org/10.1016/j.catena.2018.09.003

[64] Adeyeri, O.E., Folorunsho, A.H., Adeliyi, T.E., et al., 2024. Climate change is intensifying rainfall erosivity and soil erosion in West Africa. Science of The Total Environment. 955, 177174. DOI: https://doi.org/10.1016/j.scitotenv.2024.177174

[65] Watene, G., Yu, L., Nie, Y., et al., 2021. Spatial-temporal variability of future rainfall erosivity and its impact on soil loss risk in Kenya. Applied Sciences. 11(21), 9903. DOI: https://doi.org/10.3390/app11219903

[66] Almagro, A., Oliveira, P.T.S., Nearing, M.A., et al., 2017. Projected climate change impacts in rainfall erosivity over Brazil. Scientific reports. 7(1), 8130. DOI: https://doi.org/10.1038/s41598-017-08298-y

[67] Nasidi, N.M., Wayayok, A., Abdullah, A.F., et al., 2021. Spatio-temporal dynamics of rainfall erosivity

due to climate change in Cameron Highlands, Malaysia. Modeling Earth Systems and Environment. 7(3), 1847–1861. DOI: https://doi.org/10.1007/s40808-020-00917-4

[68] Panagos, P., Hengl, T., Wheeler, I., et al., 2023. Global rainfall erosivity database (GloREDa) and monthly R-factor data at 1 km spatial resolution. Data in brief. 50, 109482. DOI: https://doi.org/10.1016/j.dib.2023.109482

[69] Emberson, R.A., 2023. Dynamic rainfall erosivity estimates derived from IMERG data. Hydrology and Earth System Sciences. 27(19), 3547–3563. DOI: https://doi.org/10.5194/hess-27-3547-2023

[70] Abd Elbasit, M.A., Huang, J., Ojha, C.S.P., et al., 2013. Spatiotemporal changes of rainfall erosivity in Loess Plateau, China. International Scholarly Research Notices. 2013(1), 256352. DOI: https://doi.org/10.1155/2013/256352

[71] Bouderbala, D., Souidi, Z., Hamimed, A., et al., 2019. Estimation of rainfall erosivity by mapping at the watershed of macta (Algeria). Revista Brasileira de Cartografia. 71(1), 274–294. DOI: https://doi.org/10.14393/rbcv71n1-2218

[72] Singh, J., Singh, O., 2020. Assessing rainfall erosivity and erosivity density over a western Himalayan catchment, India. Journal of Earth System Science. 129(1), 97. DOI: https://doi.org/10.1007/s12040-020-1362-8

[73] Yeşilırmak, E., Atatanır, L., 2021. Variations in Erosion Risk in Western Anatolia (Turkey): Modified Fournier Approach. ÇOMÜ Ziraat Fakültesi Dergisi. 9(1), 179–188. DOI: https://doi.org/10.33202/comuagri.866697

[74] Nunes, A.N., Lourenço, L., Vieira, A., et al., 2016. Precipitation and erosivity in southern Portugal: seasonal variability and trends (1950–2008). Land Degradation & Development. 27(2), 211–222. DOI: https://doi.org/10.1002/ldr.2265

[75] Ballabio, C., Borrelli, P., Spinoni, J., et al., 2017. Mapping monthly rainfall erosivity in Europe. Science of the Total Environment. 579, 1298–1315. DOI: https://doi.org/10.1016/j.scitotenv.2016.11.123